

into a magnetic trap. After the loading process, the ^3He is pumped out by lowering the cell temperature, thereby reducing the vapor pressure of ^3He to negligible levels. Subsequent evaporative cooling could then be used to reduce the temperature of the trapped gas.

2.2. Conservative atom traps: Conservative atom traps fulfill two essential roles in BEC experiments: they keep the atoms tightly compressed during cooling, and hold the condensate for study. In principle, any trap that has a sufficiently small heating rate could be used. Conservative trapping potentials have been realized with dc magnetic fields (subsect. 2.3), ac magnetic fields [79], microwave fields [125] and far-off-resonant laser beams (sect. 8).

The requirements for the trap during cooling are more stringent than they are for holding condensates. First, the time for cooling (typically thirty seconds for evaporative cooling) is usually much longer than the time for performing experiments on BEC, requiring low heating and trap loss rates. Furthermore, for cooling, the trap needs a sufficiently high trap depth and trapping volume to hold the initial (pre-cooled) cloud, and must accommodate a cooling scheme able to reach BEC temperatures. So far, only the combination of magnetic trapping (subsect. 2.3) and evaporative cooling (subsect. 2.4) has accomplished this. Evaporative cooling has also been observed in an optical dipole trap [71], but with only a factor of 30 gain in phase-space density. Rf-induced evaporation is particularly effective and simple to implement in a magnetic trap, and perhaps this combination will become the workhorse of the nanokelvin temperature range, just as the MOT has in the microkelvin range. However, there is always room for improvement, in particular for atoms which do not have the collisional properties necessary for evaporative cooling in a magnetic trap (subsect. 2.6). Considerable progress is being made on far-off resonant trapping using blue-detuned [120, 126, 127], near-infrared [72], and CO_2 lasers [128, 129].

After cooling, trap requirements are different, and other options are available for holding the condensate. Our recent experiments on optically confined BEC (sect. 8) demonstrate that optical dipole traps confine Bose-Einstein condensates more easily than much hotter atoms. Traps for condensates can be much weaker than for laser-cooled atoms, making them easier to implement and greatly reducing heating due to beam jitter, intensity fluctuations, and spontaneous emission [130].

There are several traps which have so far not been pursued beyond their first demonstration: A microwave trap originally suggested for hydrogen atoms [131] has been realized with laser-cooled cesium atoms [125]. An ac magnetic trap for strong-field seeking atoms was suggested in 1985 [132], and realized in 1991 [79]. Finally, ac electric fields offer another possibility to trap strong-field seekers [133, 134]. All these traps are rather weak and do not seem to offer obvious advantages over the combination of optical and magnetic forces. A recent resource letter contains many references on atom traps [135].

2.3. Magnetic trapping. – The major role of the magnetic trap in a BEC experiment is to accommodate the pre-cooled atoms and compress them in order to achieve high

collision rates and efficient evaporative cooling. The steps that must be taken to obtain high collision rates, including “mode-matched” transfer and anisotropic compression, are discussed in this section. The collision rate after compression is suggested as the most important figure of merit for a magnetic trap, and will be related to the magnetic-field parameters.

Magnetic trapping of neutral atoms was first observed in 1985 [82]. Shortly afterwards, orders of magnitude improvements in density and number of trapped atoms were achieved at MIT and in Amsterdam using superconducting traps and different loading schemes [83, 121, 122]. Important aspects of magnetic trapping are discussed in [15, 45, 48, 93, 136].

Magnetic forces are strong for atoms with an unpaired electron, such as the alkalis, resulting in magnetic moments μ_m of the order of a Bohr magneton μ_B . However, it is worth pointing out that magnetic confinement was first observed for neutrons, despite their thousand-times smaller magnetic moment [137].

The interaction of a magnetic dipole with an external magnetic field is given by $-\mu_m \cdot \mathbf{B} = -\mu_m B \cos\theta$. Classically, the angle θ between the magnetic moment and the magnetic field is constant due to the rapid precession of μ_m around the magnetic-field axis. Quantum-mechanically, the energy levels in a magnetic field are $E(m_F) = g\mu_B m_F B$, where g is the g -factor and m_F the quantum number of the z -component of the angular momentum F . The classical term $\cos\theta$ is now replaced by m_F/F ; the classical picture of constant θ is equivalent to the system remaining in one m_F quantum state.

An atom trap requires a local minimum of the magnetic potential energy $E(m_F)$. For $gm_F > 0$ (weak-field seeking states) this requires a local magnetic-field minimum. Strong-field seeking states ($gm_F < 0$) cannot be trapped by static magnetic fields, because Maxwell’s equations do not allow a magnetic-field maximum in free space [80, 138].

Because magnetic traps only confine weak-field seeking states, atoms will be lost from the trap if they make a transition into a strong-field seeking state. Such transitions can be induced by the motion in the trap because an atom sees a field in its moving frame which is changing in magnitude and direction. The trap is only stable if the atom’s magnetic moment adiabatically follows the direction of the magnetic field. This requires that the rate of change of the field’s direction θ must be slower than the precession of the magnetic moment:

$$(1) \quad \frac{d\theta}{dt} < \frac{\mu_m |\mathbf{B}|}{\hbar F} = \omega_{\text{Larmor}}.$$

The upper bound for $d\theta/dt$ in a magnetic trap is the trapping frequency. This adiabatic condition is violated in regions of very small magnetic fields, creating a region of trap loss due to spin-flips to untrapped states. These spin-flips are referred to as “Majorana flops” [139].

2.3.1. Quadrupole-type traps. There are two basic types of static magnetic traps: those in which the minimum is a zero crossing of the magnetic field, and those which have a minimum around a finite field [136]. Traps with a zero-field crossing usually

generate a linear potential characterized by the gradient of the magnetic field: $B_x = B'_x x$, $B_y = B'_y y$, $B_z = B'_z z$. Maxwell's equations require that $B'_x + B'_y + B'_z = 0$. The case of axial symmetry is a spherical quadrupole field in which $B' \equiv B'_x = B'_y = -B'_z/2$. This configuration is realized with two coils in "anti-Helmholtz" configuration. This was the configuration which was first used to trap neutral atoms magnetically [82].

A linear trapping potential offers superior confinement compared to traps with a parabolic potential minimum (sub-subsect. 2'3.2). This follows from a simple argument. Coils which are a distance R_{coil} away from the trapped cloud and generate a field B_{coil} at the coil typically produce a field gradient of $B' \approx B_{\text{coil}}/R_{\text{coil}}$ and a curvature of $B'' \approx B_{\text{coil}}/R_{\text{coil}}^2$. A cloud of size r in a linear potential with gradient B' would be confined to the same size in a parabolic potential with a curvature equal to B'/r . This allows us to define an "effective curvature" of linear confinement: $B''_{\text{eff}} = B'_{\text{coil}}/r$. This exceeds the curvature of a parabolic trap by R_{coil}/r , which is usually an order of magnitude or more.

When linear traps were employed for the first demonstrations of evaporative cooling with alkali atoms [88, 89], trap loss due to Majorana spin-flips [82, 93, 139-141] near the zero of the magnetic field was encountered. For atoms moving at a velocity v , the effective size of this "hole" in the trap is $\sqrt{2\hbar v/\pi\mu_m B'}$ which is about $1 \mu\text{m}$ for $\mu_m = \mu_B$, $v = 1 \text{m/s}$ and $B' = 1000 \text{G/cm}$. As long as the hole is small compared to the cloud diameter, the trapping time can be long (even longer than a minute), and evaporative cooling in such a trap was used to increase phase-space density by more than two orders of magnitude [142]. However, as the temperature drops, the trap loss due to the hole becomes prohibitive for further cooling. Although the size of the hole depends on the thermal velocity of the atoms, and therefore shrinks as the atoms are cooled, the diameter of the atom cloud shrinks even faster with temperature, resulting in a T^{-2} dependence of the loss rate [142, 143].

Two methods have been demonstrated to plug the hole. One solution is to add a rotating magnetic bias field B_0 to the spherical quadrupole field. The frequency of the rotating field is much higher than the orbiting frequency of the atoms, but much lower than the Larmor frequency. The resulting time-averaged, orbiting potential (TOP) trap is harmonic, but much tighter than what could be obtained by dc magnets of the same size [143]. The time-averaged potential can be written as

$$(2) \quad U_{\text{TOP}} = \frac{\mu_m}{2} (B''_\rho \rho^2 + B''_z z^2),$$

$$(3) \quad B''_\rho = \frac{B'^2}{2B_0}, \quad B''_z = \frac{4B'^2}{B_0},$$

where $\rho^2 = x^2 + y^2$ is the radial coordinate.

The rotating field moves the zero of the magnetic field around in a circle (the "circle of death") of radius $r_D = B_0/B'$. Due to Majorana flops, this limits the depth of the potential to $U_{\text{TOP}}(r_D) = \mu_m B_0/4$. A large circle of death requires either large B_0 or small B' , both of which lead to weaker confinement. The TOP trap was used in the first demonstration of BEC [1]. An interesting variant of the TOP trap has been proposed,

where a rotating quadrupole field avoids the circle of death [144].

Another solution is to plug the hole using the optical dipole forces of a tightly focused blue-detuned laser beam to repel atoms from the center of the trap (see also sub-subsect. 2'5.2) [2]. The "optically plugged trap" achieves very tight confinement corresponding to a curvature of about B'/x_0 , where x_0 , the separation of the potential minimum from the zero of the magnetic field, is typically $\sim 50 \mu\text{m}$. BEC in sodium was first achieved with this trap [2].

2'3.2. Ioffe-Pritchard traps. The lowest-order (and therefore tightest) trap which can have a bias field is a harmonic trap. A magnetic trap with finite bias field along the z -direction has an axial field of $B_z = B_0 + B''z^2/2$. The leading term of the transverse field component B_x is linear, $B_x = B'x$. Applying Maxwell's equations (and assuming axial symmetry) leads to the following field configuration [136]:

$$(4) \quad \mathbf{B} = B_0 \begin{pmatrix} 0 \\ 0 \\ 1 \end{pmatrix} + B' \begin{pmatrix} x \\ -y \\ 0 \end{pmatrix} + \frac{B''}{2} \begin{pmatrix} -xz \\ -yz \\ z^2 - \frac{1}{2}(x^2 + y^2) \end{pmatrix}.$$

The parabolic trap was first suggested and demonstrated for atom trapping by Pritchard [83, 145], and is similar to the Ioffe configuration discussed earlier for plasma confinement [146]. We refer to any trap which has this field configuration as a Ioffe-Pritchard (IP) trap.

The Ioffe-Pritchard trap has two different regimes. For temperatures $k_B T < \mu_m B_0$, the cloud experiences the potential of a 3D anisotropic harmonic oscillator. In the case of $k_B T > \mu_m B_0$, the potential is predominantly linear along the radial directions ($U_\rho = \mu_m B' \rho$) and harmonic along the axial direction ($U_z = \mu_m B'' z^2/2$). As a consequence, the loss in confinement compared to a linear trap is not as severe as implied in sub-subsect 2'3.1.

For small clouds (and all condensates) the trapping potential is very well approximated by an anisotropic harmonic-oscillator potential

$$(5) \quad U \simeq \frac{\mu_m}{2} [B''_\rho \rho^2 + B''_z z^2],$$

$$(6) \quad B''_\rho = \frac{B'^2}{B_0} - \frac{B''}{2}.$$

Beyond a certain axial displacement, the radial confinement vanishes. This occurs because the radial component of the curvature term $-B''/2xz$ interferes destructively with the radial gradient B' . From eq. (4) we find that this point of instability z_{inst} occurs at

$$(7) \quad z_{\text{inst}} = \pm \left(\frac{B'}{B''} - \frac{1}{2} \frac{B_0}{B'} \right).$$

When $B_p'' \leq 0$, the instability is at the origin, and there is no radial confinement at all. The saddle point at z_{inst} requires special attention when loading large clouds into a Ioffe-Pritchard trap, as discussed in sub-subsect. 2.3.3.

The Ioffe-Pritchard trap has been used in many BEC experiments. The most straightforward implementation consists of two pinch coils and four Ioffe bars [136]. The Ioffe bars generate the radial gradient field B' , while the pinch coils produce a bias field and the curvature term B'' . Most of the bias field is usually canceled by a pair of additional “antibias” coils. By lowering B_0 , radial confinement is increased (eq. (6)). The bias field should be just high enough to suppress Majorana flops. A typical value is 1 G, although we have used values as low as 0.4 G, and smaller values are probably still stable. If the bias field is over-compensated, the field will cross zero and Majorana flops will occur (fig. 3). Since both the pinch coils and the antibias coils can produce fields on the order of 500 to 1000 G, the cancellation has to be carefully controlled. We achieved best results when both sets of coils were powered in series by the same power supply, and fine bias adjustments were made by carefully moving a few loops of the antibias coils.

Since the pinch coils and the Ioffe bars are very close to the atoms, this configuration is very efficient in producing a tight trapping potential. It has been used in several BEC experiments [4, 147]. The optical access can be improved by elongating the pinch coils, or using a cloverleaf configuration [148] (fig. 4) where the Ioffe bars are removed, and the radial field gradient is created by a pair of four coils surrounding each pinch coil. This configuration is used in several experiments because it has open, 360° access in the x - y plane, and the coils may be placed outside the vacuum chamber. Some simpler winding patterns (baseball [25, 136], yin-yang [136], three-coil [149, 150], four-dee [102]) do not allow for independent control of B' and B'' , although the radial confinement can still be varied through B_0 . Other implementations of the Ioffe-Pritchard trap include permanent magnet traps [3, 151], and traps with ferromagnetic pole pieces [152].

2.3.3. Mode matching. Evaporative cooling can increase phase-space density by many orders of magnitude as long as the atoms rethermalize quickly compared to the trap lifetime. This makes the collision rate during cooling even more important for BEC than the initial phase-space density of the pre-cooled atoms. In order to maximize the collision rate, atoms are transferred into an optimized (“mode matched”) magnetic trap, and then adiabatically compressed.

“Mode matching” between an atom cloud and a trap is achieved when the transfer of atoms maximizes phase-space density. This also optimizes the elastic collision rate which will be achieved after compressing the trap (sub-subsect. 2.3.4), because all properties of the compressed cloud, including the collision rate, are completely determined by the number of atoms N and the phase-space density \mathcal{D} . Adiabatic compression conserves N and \mathcal{D} , so a loss in phase-space density when loading the magnetic trap corresponds to an equal loss in the compressed trap. For a power law potential $U(r) \propto r^{d/\delta}$ in d dimensions, the volume of a cloud at temperature T scales as $V \propto T^\delta$. The collision rate

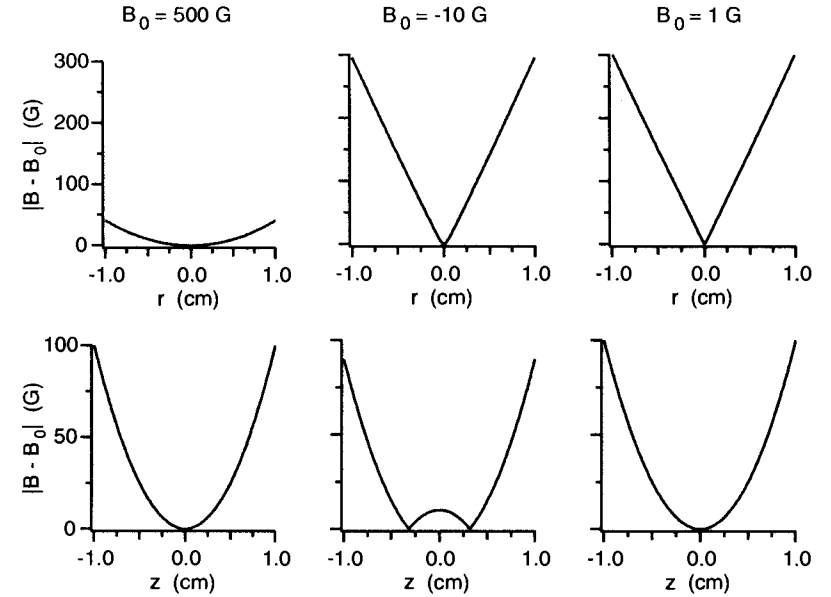


Fig. 3. Bias field compensation in an Ioffe-Pritchard trap is important for tight radial confinement. The magnetic field in an IP trap characterized by a radial gradient of 300 G/cm and an axial curvature of 200 G/cm² is shown for three bias fields B_0 . The upper row displays radial cuts, and the lower row displays axial cuts of the magnetic-field profile. In the first column, radial confinement is softened as a result of the large bias field. In the second column, the bias field is over-compensated, resulting in a pair of zero-field crossings along the axis of the trap. In the third column, the bias field is tuned correctly, resulting in tight radial confinement and no zero-field crossings.

Γ_{el} for atoms with a collisional cross-section σ and a thermal velocity v is equal to

$$(8) \quad \Gamma_{\text{el}} = n\sigma v \propto \mathcal{D}^{\frac{\delta-1/2}{\delta+3/2}} N^{\frac{2}{\delta+3/2}}.$$

In particular, for a 3D harmonic trap ($\delta = 3/2$), the collision rate is proportional to $\mathcal{D}^{1/3}$. This implies that the loss in collision rate due to non-ideal transfer is much less severe than the loss in phase-space density.

Atoms are transferred into a magnetic trap by suddenly switching off the MOT, applying polarization gradient cooling for a few milliseconds, and then suddenly turning on the magnetic trap and building a new potential around the atoms. When transferring a spherical, Gaussian shaped cloud of atoms with an rms radius r_0 and temperature T into a harmonic trap, phase-space density is conserved if the potential $(1/2)\kappa r^2$ has a stiffness $\kappa = \kappa_0 = k_B T / r_0^2$. This will ensure that the atoms maintain their volume and

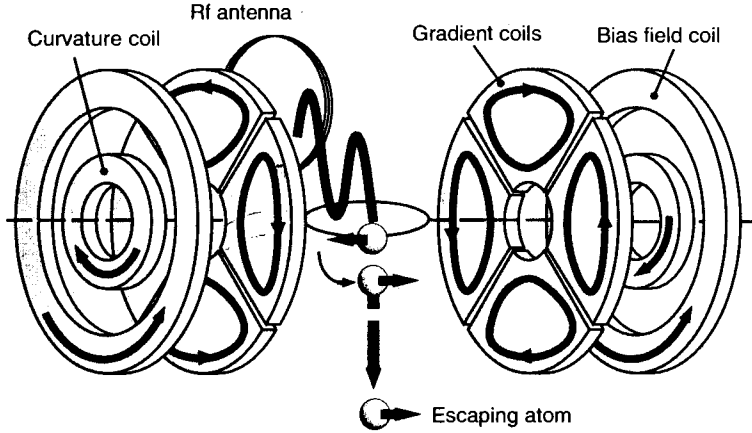


Fig. 4. – In a cloverleaf trap, Ioffe bars are replaced by eight “cloverleaf” coils surrounding the pinch coils, providing 360 degree optical access. Evaporation is done by selectively spin-flipping atoms into untrapped states with rf radiation.

temperature. If the trap is too tight, the atoms will be heated by the transfer. If it is too loose, the atoms will expand non-adiabatically. In either case phase-space density will be lost. For ideal loading we have used the term “mode matching”, in analogy with the coupling of a laser beam into a single-mode fiber, where the efficiency suffers from focusing which is either too weak or too tight.

If the magnetic trap is not mode-matched, *i.e.* $\kappa \neq \kappa_0$, then the phase-space density \mathcal{D} is reduced from its initial value \mathcal{D}_0 [153]:

$$(9) \quad \frac{\mathcal{D}}{\mathcal{D}_0} = \frac{8 \left(\frac{\kappa}{\kappa_0} \right)^{3/2}}{\left(1 + \frac{\kappa}{\kappa_0} \right)^3}.$$

This loss is only a weak function of mode mismatch. For example, the phase-space density decreases only by half when κ is four times larger or smaller than κ_0 . More importantly, the collision rate is still 80% of its maximum value.

Mode matching into a Ioffe-Pritchard trap is done with a high bias field ($\mu_m B_0 > k_B T$). This requires (eq. (6))

$$(10) \quad B'' = \frac{\kappa_0}{\mu_m},$$

$$(11) \quad \frac{B'^2}{B_0} = \frac{3\kappa_0}{2\mu_m}.$$

It is important that the initial cloud radius r_0 be much smaller than the distance to the trap instabilities (eq. (7)), otherwise, atoms will spill out of the trap. Inserting eqs. (10) and (11) into eq. (7) gives an instability distance of $z_{\text{inst}} = \sqrt{B_0(2\mu_m/3\kappa_0)} = B'(2\mu_m/3\kappa_0)$. This shows that both a large bias field and a large gradient are necessary, which is unfortunate because this requires a fast rise time of the high-current power supplies.

For $\mu_m B_0 < k_B T$, the radial confinement is linear, and mode matching would require $\mu_m B' \approx k_B T/r_0$. With this condition we find that $z_{\text{inst}} \approx r_0$, and therefore mode matching cannot be done at low bias field.

2.3.4. Adiabatic compression. Adiabatic compression plays a crucial role in BEC experiments because it increases the collision rate before evaporative cooling. In our first BEC demonstration [2] adiabatic compression increased the collision rate by a factor of 20, resulting in BEC after only 7 seconds of evaporative cooling!

If, after loading, the potential (again characterized by a volume $\propto T^\delta$) is adiabatically increased by a factor α , the temperature rises by a factor $\alpha^{2\delta/(2\delta+3)}$ and the density by $\alpha^{3\delta/(2\delta+3)}$. Phase-space density is constant, but the elastic collision rate increases by a factor $\alpha^{4\delta/(2\delta+3)}$ as long as the cross-section is constant.

Adiabaticity requires

$$(12) \quad \frac{d\omega_{\text{trap}}}{dt} \ll \omega_{\text{trap}}^2.$$

Violation of adiabaticity, however, does not have severe consequences. If the compression is done suddenly in a harmonic trap ($\delta = 3/2$), the collision rate increases by a factor $2\alpha^{3/2}/(1+\alpha)$ rather than α . For a sudden compression by a factor of five, one still reaches 75% of the maximum possible collision rate. Note that this is the same loss we would see if we transferred atoms into a trap which was mode-mismatched by a factor α (eq. (9)). Non-mode-matched transfer is equivalent to a mode-matched transfer plus a sudden (de-)compression to the same potential strength.

Compression in an Ioffe-Pritchard trap involves one more complication. Initially, the aspect ratio is adjusted to ≈ 1 to ensure mode-matched loading of a spherical cloud. This requires a high bias field B_0 . Subsequent compression includes lowering the bias field to achieve the maximum radial confinement. This process elongates the cloud into a cigar shape. In addition to the usual adiabaticity criterion (12), the compression has to be slow compared to the elastic collision rate. Otherwise, the anisotropic compression would lead to an anisotropic temperature and subsequent loss of phase-space density during equilibration.

Anisotropic heating is hard to avoid when the initial collision rate is low. Fortunately, nature is forgiving. Radial compression by a factor of α causes the temperature to rise by a factor of $\alpha^{1/3}$ if done adiabatically, and by a factor of $(2\sqrt{\alpha} + 1)/3$ (after rethermalization) if done suddenly. Since the elastic collision rate is inversely proportional to temperature in a given 3D harmonic-oscillator potential, one still obtains 94% of the

maximum possible collision rate when a 2D compression by a factor of $\alpha = 5$ is done quickly with respect to the thermalization rate.

Furthermore, the radial compression in a Ioffe-Pritchard trap usually takes us to the small bias field regime ($B_0 < k_B T / \mu_m$), changing the radial confinement from harmonic to linear. As pointed out by Pinkse *et al.* [154] and discussed in subsect. 8.2, this increases the phase-space density by a factor of e . This increase is due to collisions which change the population of energy levels, but conserve entropy.

When the bias field B_0 is lowered adiabatically, the collision rate Γ increases by

$$(13) \quad \frac{\Gamma_{\text{final}}}{\Gamma_{\text{initial}}} = \frac{e^{1/2}}{2} \left[\frac{\mu_m B_{0\text{initial}}}{k_B T_{\text{initial}}} \right]^{1/2}.$$

We can apply estimates for adiabatic compression in a harmonic trap to linear potentials by noting that B' confines a cloud at the same temperature and density as a harmonic trap with magnetic-field curvature $B''_{\text{equiv}} = B'/r = B'^2/k_B T$, where r characterizes the size of the cloud. If we use this equivalent curvature to characterize the compressed trap, we get the same result as eq. (13) – apart from the factor $e^{1/2}/2$. This emphasizes that lowering the bias field beyond a value $k_B T / \mu_m$ does not compress the cloud any further.

2.3.5. Figure of merit for magnetic traps. The major goal when designing magnetic traps for BEC experiments is to get the highest collision rate after compression. Therefore, we regard this as the figure of merit of a trap. In a 3D harmonic oscillator, the collision rate increases due to adiabatic compression in proportion to the geometric mean of the three curvatures: $(B''_x B''_y B''_z)^{1/3}$.

In an Ioffe-Pritchard trap, after full compression to a final temperature T , the equivalent radial curvature is $\mu_m B'^2 / k_B T$. Knowing that the final temperature scales with the geometric mean of the trapping frequencies, we find that the collision rate will depend on $B' B''^{1/4}$, implying that it is much more important to have strong-field gradients than curvatures.

Let us compare this result to a TOP trap, assuming that the TOP trap is compressed until the trap depth due to the circle of death is $5k_B T$, a typical barrier for evaporative cooling. In this case, the effective radial curvature is

$$(14) \quad B''_{\text{TOP},r} = \frac{\mu_m B'^2}{40k_B T}.$$

This implies that the TOP trap corresponds to an IP trap with a $\sqrt{40}$ smaller value of B' . Along the axial direction, the effective curvature B'' of a TOP trap is typically 100 times larger than that of an IP trap. The figure of merit, $B' B''^{1/4}$, is slightly higher for an IP trap, but this does not take into account the fact that one can usually obtain higher gradients in spherical quadrupole traps than in IP traps.

If we wish to compare the confinement for condensates after cooling, the effective radial curvatures of TOP traps and IP traps are $B'^2/2B_0$ and B'^2/B_0 , respectively. The maximum confinement depends on how small B_0 can be, as determined by the adiabatic

condition which ensures stability of the trap (eq. (1)). Usually B_0 is smaller in IP traps than in TOP traps, because the use of time-dependent fields in the TOP trap requires larger Larmor frequencies to prevent non-adiabatic spin-flips. However, experiments have not yet explored the lower limits for B_0 in either type of trap (see [155] for a theoretical treatment).

The bottom line is that both traps work very well. The TOP trap might have advantages in studying vortices due to the built-in rotation, and does not require careful bias-field cancellation. The advantages of the IP trap are the variable aspect ratio and the use of only dc fields. Several groups have now built magnetic traps using room temperature electromagnets which provide sufficient confinement for evaporation to BEC. Even tighter confinement, and therefore faster evaporation, could be achieved with permanent magnets or superconducting magnets, but at the price of less flexibility.

2.4. Evaporative cooling. Gaseous Bose-Einstein condensates have so far only been obtained by evaporative cooling. Evaporative cooling is done by continuously removing the high-energy tail of the thermal distribution from the trap. The evaporated atoms carry away more than the average energy, which means that the temperature of the remaining atoms decreases. The high energy tail must be constantly repopulated by collisions, thus maintaining thermal equilibrium and sustaining the cooling process. Evaporative cooling is a common phenomenon in daily life – it is how hot water cools down in a bathtub or in a cup of coffee. Evaporative cooling of trapped neutral atoms was developed at MIT as a method for cooling atomic hydrogen which had been pre-cooled by cryogenic methods [53,54,156]. The first suggestion by Hess [53] was soon followed by an experimental demonstration [54]. Evaporative cooling has been reviewed in [15,48], and we only briefly summarize the basic aspects here.

The essential condition for evaporative cooling is a long lifetime of the atomic sample compared to the collisional thermalization time. Trapped atom clouds are extremely dilute (about ten orders of magnitude less dense than a solid or a liquid) and collisional thermalization can take seconds. A major step was taken in May 1994 when the MIT and JILA groups combined laser cooling with evaporative cooling, extending the applicability of evaporative cooling to alkali atoms [88,89].

In these experiments, the evaporation of atoms was controlled by radio frequency radiation (rf-induced evaporation). This technique was proposed by Pritchard [81] and Walraven [157] and first demonstrated by our group when spatial truncation of magnetically trapped atoms was observed [158]. Increases in phase-space density were reported by the MIT and Boulder groups at IQEC in May 1994 and at ICAP-XIV [88,89] and published after further progress had been achieved [142,143]. Other early work on evaporation of alkali atoms was done at Rice [90] and Stanford [71].

In rf-induced evaporation, the rf radiation flips the atomic spin. As a result, the attractive trapping force turns into a repulsive force and expels the atoms from the trap (fig. 4). This scheme is energy-selective because the resonance frequency is proportional to the magnetic field, and therefore to the potential energy of the atoms. In the case of transitions between magnetic sublevels m_F , the resonance condition for the